

Product State Distributions from the Reaction $O(^3P) + HBr$

Kenneth G. McKendrick, David J. Rakestraw and Richard N. Zare*

Department of Chemistry, Stanford University, Stanford, California 94305, U.S.A.

An experimental investigation has been performed of the hydrogen atom abstraction reaction $O(^3P) + HBr \rightarrow OH(X^2\Pi) + Br$. A photolytic method was used to produce $O(^3P)$ in the presence of HBr, and laser-induced fluorescence detection employed to obtain the nascent vibrational, rotational and fine-structure state partitioning in the product OH. Distributions were found to be highly internally excited, with a strong vibrational inversion and substantial rotational excitation, extending to the limit of available energy. Non-statistical distributions of the fine-structure states were observed. The possibility of a subsidiary reactive channel producing spin-orbit excited $Br(^2P_{1/2})$ is proposed as an explanation for an apparent anomaly in the $OH(v''=1)$ rotational distribution. The dynamics generally appear consistent with the kinematic constraints imposed by the heavy + light-heavy mass combination.

Considerable experimental and theoretical effort has been expended in attempting to understand the roles of kinematic constraints and potential-energy surfaces in governing reactivity and the partitioning of available energy in the products of chemical reactions. Hydrogen atom abstraction by a heavy atom from the hydride of a second heavy atom (or molecule) constitutes an important example of the class of reactions characterised by a heavy + light-heavy ($H + LH'$) mass combination. In those exothermic $H + LH'$ reactions thought to proceed *via* direct abstraction, it has generally been found,^{1–12} with some exceptions,^{13–21} that kinematic constraints dominate over potential surface effects, causing substantial excitation of both rotational and vibrational degrees of freedom of the products.

The majority of hydrogen atom abstraction reactions of ground-state atomic oxygen, $O(^3P)$, fall into the $H + LH'$ category, and are furthermore of immense practical importance because of their involvement in many combustion and atmospheric processes. Experimental investigations of the dynamics of the reactions of $O(^3P)$ with a wide variety of organic molecules have revealed^{13–19} that a substantial proportion of the available energy is released as OH product vibration, but, uncharacteristically, that very little rotational excitation is imparted to OH. These results have been satisfactorily reproduced by quasiclassical trajectory (QCT)²⁰ and vibrationally adiabatic distorted-wave (VADW)²¹ calculations, on a semiempirical London–Eyring–Polanyi–Sato (LEPS) potential-energy surface, constructed²⁰ to yield computed results consistent with certain limited aspects of the experimental data.

No equivalent, detailed dynamical information has hitherto been reported for the reaction of $O(^3P)$ with an inorganic hydride, the generally smaller reaction cross-section making such a study technically more challenging. Extensive kinetic investigations of the reactions with the hydrogen halides have been performed,^{22–24} including reaction with vibrationally excited HCl,^{25–29} and some information on vibrational branching in the OH product is available from infrared chemiluminescence measurements on $O + HI$,⁶ e.s.r. studies of $O + HBr$,⁵ and laser-induced fluorescence (LIF) detection of the OH produced in the reaction of $O(^3P)$ with vibrationally excited HCl.²⁹

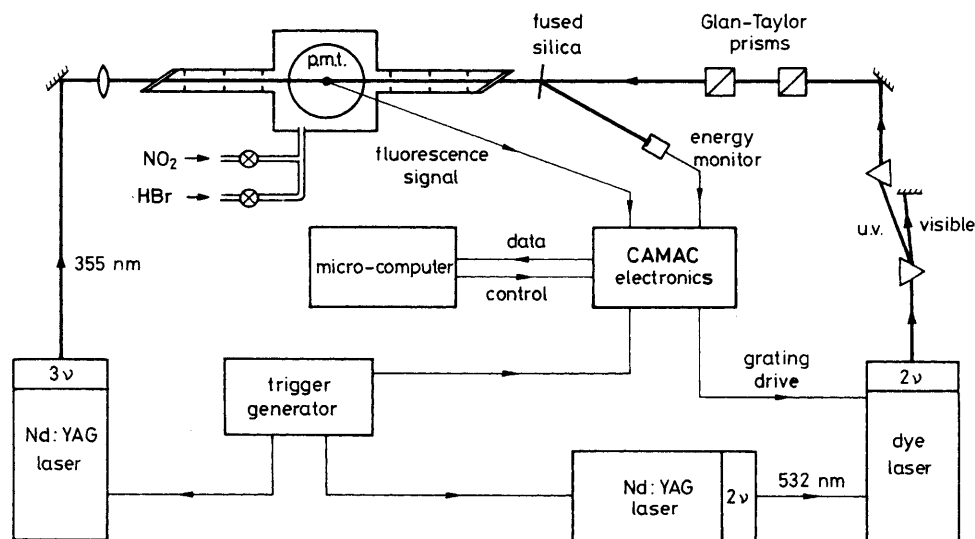


Fig. 1. Schematic diagram of the apparatus for counter-propagating 'pump-probe' laser photolysis, laser-induced fluorescence experiments.

The subject of this paper is an experimental investigation of the vibrational and rotational product state distributions in the exothermic reaction



An activation barrier of 14 kJ mol^{-1} has been deduced from kinetic studies,²⁴ leading to relatively slow reaction at room temperature [$k(O + HBr) = 3.4 \times 10^{-14} \text{ cm}^3 \text{ molecule}^{-1} \text{ s}^{-1}$]. A very strong vibrational inversion was observed in the OH product in the e.s.r. experiments of Spencer and Glass,⁵ but no rotational information was extractable, given the highly collisional flow-tube conditions.

The experimental method of this study involves the generation of $O(^3P)$ by 355 nm photolysis of NO_2 in the presence of HBr. The nascent OH product is detected in a state-specific fashion by excitation of LIF on the well known $A^2\Sigma^+ - X^2\Pi$ transition,³⁰ at a short delay following the photolysis pulse.

The principal question which will be addressed is whether the dynamics of this reaction are similar to those of hydrogen atom abstraction from organic molecules, or, conversely, more closely related to those of the majority of $H + LH'$ systems. An early collinear quantum-mechanical study of this system³¹ must now be considered suspect in the light of subsequent criticism.⁸ Very recently, Persky and coworkers,⁹ in one of a series of theoretical papers on the dynamics of $O(^3P) + \text{hydrogen halide reactions}$,^{7,10} have reported the results of a quasiclassical trajectory study on a semiempirical LEPS $O + HBr$ surface, optimised to produce agreement with the available kinetic data. The predictions of this QCT study are compared with the new experimental results which we have obtained, and the validity of the proposed potential-energy surface discussed.

Experimental

A schematic diagram of the apparatus is shown in fig. 1, depicting the counter-propagating 'pump-probe' geometry of the experiment. A steadily flowing mixture of HBr and NO_2 was maintained in the stainless-steel reaction chamber, exhausted by a partially throttled diffusion pump. The pressure was monitored by a capacitance manometer

(MKS Baratron 222BA, 0–10 Torr, † absolute). The photolysis ('pump') beam consisted of 355 nm light produced by third harmonic generation of the output of a Nd:YAG laser (Quantel 581), brought to a loose focus (spot-size *ca.* 2 mm) at the centre of the chamber. Pulse energies were typically 20 mJ. Laser-induced fluorescence was excited by tunable ultraviolet ('probe') radiation in the 280–360 nm region produced by a Nd:YAG (Quanta Ray DCR-2A) pumped dye laser (Quantel TDL-50) combination, with a spectral bandwidth of *ca.* 0.2 cm^{-1} . Both pump and probe lasers were operated at a repetition frequency of 20 Hz. The probe beam spot-size (5 mm) was arranged to be sufficiently greater than that of the pump beam to ensure the detection of all species produced at the short time delays between laser pulses employed in the experiments. Great care was taken to account fully for the effects of radiative saturation of the OH *A*-*X* transition:³² probe pulse energies were reduced by a combination of Glan-Taylor prisms (which allow variable attenuation while maintaining a fixed polarisation). These energies were monitored on a shot-to-shot basis *via* a partial reflection from a quartz plate, at near normal incidence, onto a power meter (Molelectron J3-05). The laser beams propagated through internally baffled entrance and exit arms (1 m long), and all internal surfaces were coated with a matt black paint (Zuel Corporation, St Paul, MN), greatly reducing the level of scattered laser light.

Fluorescence was collected in the vertical direction, perpendicular to the common axis of the laser beams, by a fused silica lens system ($f = 5\text{ cm}$), and imaged through an interference filter (chosen to transmit the desired vibronic band of the OH *A*-*X* system) onto the photocathode of a photomultiplier tube (Centronic 4283/81). Signals were captured during a gate of length $1.5\ \mu\text{s}$ (corresponding to approximately twice the radiative lifetime of OH *A* $^2\Sigma^+$), delayed by *ca.* 20 ns from the probe pulse to discriminate against scattered laser light. The digitised data (LeCroy 2249SG ADC, CAMAC modular data bus) were passed to a microcomputer (IBM PC-XT) for storage and analysis.

Gases used had the following stated purities: HBr (Matheson, >99.8%), HCl (Matheson, >99.0%) and NO₂ (Matheson, >99.5%). The NO₂ reservoir was maintained at 0 °C to ensure a stable backing pressure.

Results

Preliminary measurements were performed to identify conditions under which an authentic nascent product state distribution would be observed. The majority of these initial investigations probed the OH($v'' = 1$) rotational distribution, the signals being most intense for this vibrational level. Relaxation of this distribution could readily be observed as the product of the pressure, *P*, in the chamber and the delay time, Δt , between the photolysis and probe laser pulses was increased. As has previously been observed,³³ the lowest rotational states were most rapidly relaxed, with the higher levels being relatively metastable. It was found that the measured OH($v'' = 1, J''$) distribution was essentially invariant for values of $P\Delta t < 4 \times 10^{-8}\text{ Torr s}$. Data were generally collected at $P\Delta t = 2 \times 10^{-8}\text{ Torr s}$. Furthermore, it was also found that the distribution was insensitive to the total pressure, for a given value of $P\Delta t$, in the pressure range 0–80 mTorr, indicating the absence of substantial variation in the fluorescence quenching rates of different rotational states in OH(*A* $^2\Sigma^+$) for the present colliding species (generally present in the ratio 1:1, HBr:NO₂). (Such effects have previously been observed for certain quencher molecules.³⁴)

The OH *A*-*X* diagonal vibronic transitions may readily be radiatively saturated with the probe pulse energies available from the present dye-laser system. To determine the

† 1 Torr = 101 325/760 Pa.

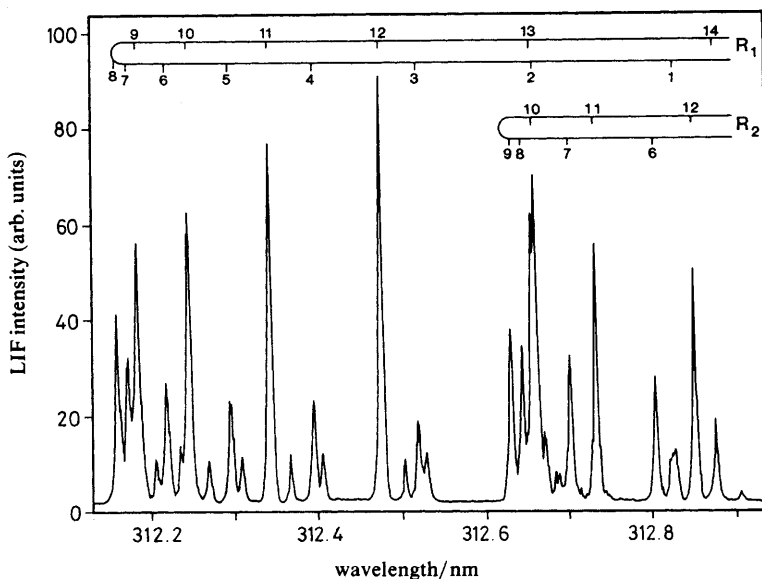


Fig. 2. LIF excitation spectrum of the OH A-X (1, 1) band from the reaction $O + \text{HBr}$. Fluorescence was selectively detected on the (1, 0) band. Conditions: 25 mTorr HBr, 25 mTorr NO_2 ; pump pulse-to-probe pulse delay of 500 ns; probe pulse energy of $150 \mu\text{J}$.

regime where the LIF signal would be linearly proportional to the probe pulse energy, measurements were made of the ratios of intensities of main branch lines to those of corresponding satellite branches (e.g. P_2 and P_{12} , or Q_1 and Q_{21}). These pairs of lines probe the same lower state, but with substantially different transition probabilities. From a knowledge of these transition probabilities, which have been accurately calculated,³⁵ the extent of any radiative saturation could be estimated.³² It was found that for excitation on the $A^2\Sigma^+$, $v' = 1 - X^2\Pi$, $v'' = 1$ band [henceforth denoted $(v', v'') = (1, 1)$], pulse energies $< 10 \mu\text{J}$ produced essentially linear response, in good agreement with expectations from the absolute transition probability³⁵ and the spatial and temporal characteristics of the probe beam. For the significantly weaker off-diagonal (0, 1) and (1, 2) transitions, pulse energies of $< 500 \mu\text{J}$ were correspondingly found to be adequate for linear response.

Measured Distributions

$\text{OH}(v'' = 1, 2)$

The $\text{OH}(v'' = 1)$ distribution was obtained by recording laser-excitation spectra (fluorescence intensity as a function of probe laser wavelength) excited on the (1, 1) transition. Fluorescence was observed only on the (1, 0) transition (through an interference filter centred at 280 nm), eliminating any possible congestion of the spectrum from the excitation of (0, 0) transitions lying in the same wavelength region, and reducing the level of observed scattered laser light.

A representative spectrum, containing the R-branch region of the (1, 1) band, is presented in fig. 2. Substantial rotational excitation is readily discerned, with well formed R_1 - and R_2 -branch bandheads. The maximum intensities occur in the returning, higher rotational lines. The rotational substate populations were obtained from analysis of this and other similar spectra, many of which were obtained at reduced probe pulse

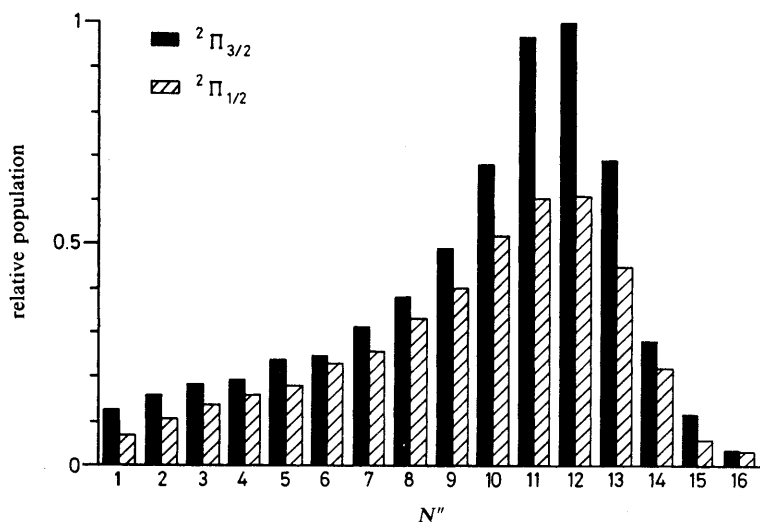


Fig. 3. Relative rotational state populations in ${}^2\Pi_{3/2}$ (solid bars) and ${}^2\Pi_{1/2}$ (hatched bars) fine structure components of $\text{OH}(v''=1)$ formed in the reaction $\text{O} + \text{HBr}$.

energies (see above), including data for all of the six main spectroscopic branches. The analysis incorporated appropriate corrections for variations in the probe pulse energy, account of the wavelength dependence of the interference filter transmission, and application of the small, well known polarisation corrections required when exciting LIF with a linearly polarised laser.³⁶ (Derived populations were not sensitive to the relative directions of linear polarisation of the pump and probe lasers.) Fig. 3 shows the resulting distributions of the ${}^2\Pi_{3/2}$ and ${}^2\Pi_{1/2}$ states as a function of N'' (the total rotational angular momentum quantum number excluding electron spin). The sharply peaked, highly excited character of the distribution is apparent.

Similarly, the $\text{OH}(X\ {}^2\Pi, v''=2)$ rotational substate distribution was obtained by pumping the off-diagonal (1, 2) transition. In this case, two possible detection schemes were exploited, using interference filters to detect selectively fluorescence on either the (1, 0) or (1, 1) bands. Signals on the (1, 0) band were weaker than those on (1, 1), the radiative transition probability being smaller,³⁵ compounded by a (purely instrumental) lower detection sensitivity. However, the spectrum is simplified by being uncongested by overlapping lines from other bands. Conversely, the detection scheme involving (1, 2) excitation followed by (1, 1) fluorescence detection results in simultaneous observation of LIF excited from $v''=1$ on the (0, 1) band, and emitted on the (0, 0) band. The alternative approaches thus provide complementary information; a more complete distribution is obtained from detection of (1, 0) fluorescence, but simultaneous observation of fluorescence on the diagonal bands allows the vibrational branching ratio $v''=1/v''=2$ to be determined, in addition to providing partial confirmation of the $v''=2$ rotational distribution.

Fig. 4 shows a representative laser-excitation spectrum of the 348–350 nm region, with fluorescence observed on the diagonal bands. Lines originating from $v''=1$ and $v''=2$ are indicated in the figure. Conditions were once again such that a nascent distribution is believed to have been observed. From this spectrum and similar data, including observations of the (1, 0) fluorescence, the rotational substate populations in $v''=2$ were derived (see fig. 5). Corrections similar to those described for the $v''=1$ data were applied. It can be seen that the $v''=2$ rotational distribution is also substantially excited, but less so than that of $v''=1$.

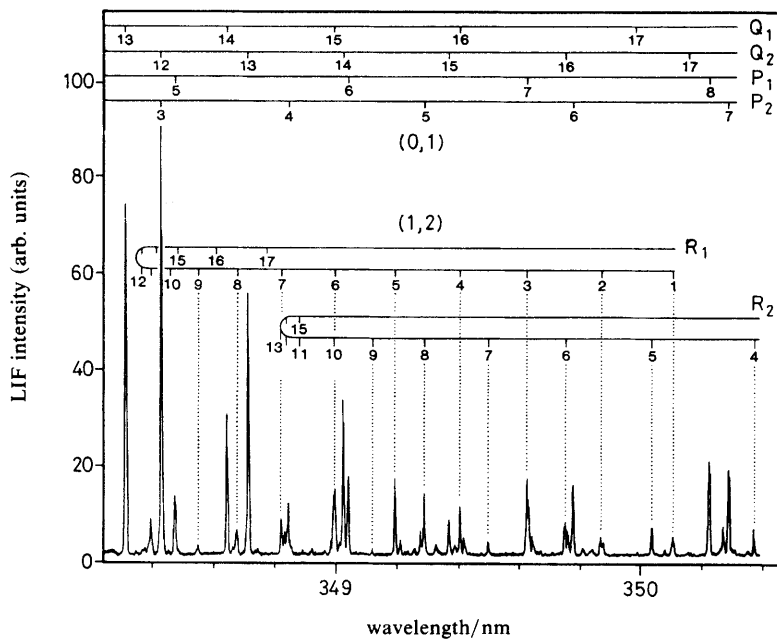


Fig. 4. LIF excitation spectrum of the OH A-X (0, 1) and (1, 2) bands from the reaction $O + \text{HBr}$. Fluorescence was observed on the (0, 0) and (1, 1) diagonal bands. Transitions originating from $v'' = 2$ are explicitly indicated by dotted lines. Experimental conditions were: 50 mTorr HBr, 50 mTorr NO_2 ; pump pulse-to-probe pulse delay of 200 ns; probe pulse energy of $700 \mu\text{J}$.

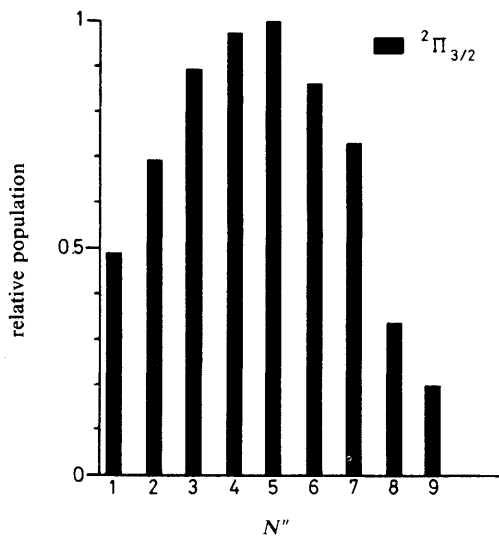


Fig. 5. Relative rotational state populations in the $^2\Pi_{3/2}$ fine structure component of $\text{OH}(v'' = 2)$ produced in the reaction $O(^3P) + \text{HBr}$.

OH($v'' = 0$)

Attempts were also made to observe any possible production of OH($v'' = 0$) from the reaction O + HBr. Significant $v'' = 0$ LIF signals were obtained by pumping and detecting on the (0, 0) transition. However, these signals were found to be entirely 'prompt', with no kinetic accumulation (of the order of a few μs) of the OH population following the photolysis pulse, as had been observed for the higher vibrational states. Examination of the $v'' = 0$ rotational state distribution revealed it to be identical to that reported³⁷ for OH produced in the photolysis of HONO at 355 nm. The magnitude of this signal could be substantially reduced by increasing the flow rate of gases through the reaction chamber while maintaining a constant pressure, once gain in contrast to the $v'' = 1$ and 2 data, which were independent of the flow rate (except, as might be expected, at very low flows). It was concluded that OH($v'' = 0$) was arising through heterogeneous production and subsequent photolysis of HONO.

Although previous reports³⁷ have indicated the absence of any significant production of higher vibrational states of OH in the 355 nm photolysis of HONO, a control experiment was performed to provide confirmation that the distributions ascribed to products of the O + HBr reaction were not distorted by a contribution from HONO photolysis. Photolysis of a flowing mixture of HCl and NO₂ was found to generate OH($v'' = 0$) with a rotational state distribution identical to that from photolysis of HBr-NO₂. The relative magnitudes of the OH($v'' = 0$) signals were taken as a measure of the HONO concentration, allowing an assessment to be made of the contribution of HONO photolysis to the observed OH($v'' = 1$) signal from HBr-NO₂. No OH($v'' = 1$) was observable, above the residual noise level, following photolysis of HCl-NO₂ mixtures, constraining this estimate to be an upper limit. It was consequently concluded that HONO photolysis could not be responsible for a contribution of >5% to the population of the lowest rotational states of OH($v'' = 1$), where such an effect would be expected to be most significant.

Vibrational Branching Ratio

As discussed above, measurements such as those displayed in fig. 4 allow an estimate to be made of the vibrational branching ratio $v'' = 1/v'' = 2$. Total populations in each of the vibrational states were calculated by summing over all rotational substates (each of the Λ -doublet components of each of the spin-orbit states). Those state populations not measured because of spectroscopic congestion were estimated by interpolation of the available data. Einstein coefficients used in obtaining the branching ratio were the experimentally determined values of Copeland *et al.*³⁸ The statistical accuracy of the population measurements was relatively high, *ca.* 10%, and the major source of uncertainty in the branching ratio therefore arose from the quoted uncertainties³⁸ in the Einstein coefficients. The derived vibrational branching ratio was OH($v'' = 1$)/OH($v'' = 2$) = 9.4 ± 3.1 at the 95% confidence level, assuming no other sources of systematic error.

The significant background OH($v'' = 0$) population resulting from HONO photolysis prevented any rigorous assessment of the branching into $v'' = 0$ of the OH product from O + HBr. However, the observed rotational distributions for $v'' = 1$ and 2 exhibit a strong propensity for population of states which are approximately thermoneutral with respect to the reagents (as will be discussed further below). It therefore seems a reasonable assumption, as is supported by the results of the quasiclassical trajectory study of Persky and co-workers,⁹ that any OH($v'' = 0$) produced in the reaction would occupy relatively high rotational states, peaking in the range $N'' = 14$ –18. The OH($v'' = 0$) rotational distribution from 355 nm photolysis of HONO is relatively 'cold', with very little population in these higher levels. We observed no significant secondary maximum in this distribution, and estimate, on the basis of the above assumption, that $v'' = 0$ constitutes <10% of the total population from the reaction O + HBr. This observation is

consistent with the results of the previous e.s.r. study of Spencer and Glass,⁵ where >97% of the OH produced was estimated to have been formed in $v'' = 1$.

Fine Structure and Λ -Doublet Population Ratios

The OH $^2\Pi$ ground state is subject to the well known spin-orbit and Λ -doublet splittings, resulting in four spin substates for each quantum number, N'' . The lower and upper spin-orbit states are labelled $^2\Pi_{3/2}$ and $^2\Pi_{1/2}$, respectively. These levels are split by *ca.* 125 cm^{-1} at the lowest rotational state, but this splitting decreases quite rapidly with increasing N'' as the character of the angular momentum coupling changes from Hund's case (a) towards case (b).

There has been considerable confusion and contradiction in the use of π^+ and π^- as labels for Λ -doublet states. An exposition of the directional nature of the electronic charge distribution of Λ -doublets was recently presented by Andresen and Rothe,³⁹ but unfortunately did not resolve the residual contradictions of nomenclature in many prior and, indeed, subsequent papers. We have therefore chosen to adopt a notation whereby $\pi(\parallel J)$ denotes states which, in the limit of large rotational angular momentum, J , have the unpaired $p\pi$ electron lobe parallel to J ; correspondingly, $\pi(\perp J)$ refers to those states with the $p\pi$ lobe perpendicular to J , and hence in the plane of rotation of the molecule. For a Σ - Π transition, such as in the present case for OH, $\pi(\parallel J)$ states are probed by Q-branch lines, and $\pi(\perp J)$ states by P- and R-branch lines.

As can be seen from the $^2\Pi_{3/2}$ $\pi(\perp J)$ and $^2\Pi_{1/2}$ $\pi(\perp J)$ populations of OH($v'' = 1$) presented in fig. 3, a preference of *ca.* 30% for the lower spin-orbit state was observed. A similar preference was found in the $v'' = 2$ data. The spin-orbit ratio is obtained from data taken on branches with very similar line strengths and equivalent polarisation properties, and seems unlikely to be subject to systematic errors of this magnitude.

The Λ -doublet ratio was less well defined. Near the peak of the $v'' = 1$ distribution, with N'' in the range 10–12, a reproducible, weak preference was found, with a maximum discrepancy of *ca.* 25% in favour of the $\pi(\perp J)$ component at $N'' = 10$. The ratio was found to vary with N'' , being insignificantly different from unity for $N'' > 13$ and $N'' < 7$. (It is required that the states be equally populated in the limit of no nuclear rotation, since there can be no degree of electron alignment.) We hesitate to attach too great a significance to the observed weak preference, it being close to the level of systematic uncertainty in comparing data taken on branches with substantially different line strengths and polarisation properties. The $v'' = 2$ data similarly showed little preference for either Λ -doublet component.

Discussion

A diagram showing reagent and product state energetics in the $O + HBr$ system is presented in fig. 6. Fine structure states in $O(^3P)$ and $OH(X^2\Pi)$ are not indicated: only the lowest-energy $O(^3P_2)$ and $OH(X^2\Pi_{3/2})$ states are shown. Channels leading to ground, $^2P_{3/2}$, and excited, $^2P_{1/2}$, spin-orbit states of the bromine atom, separated by 3685 cm^{-1} , are denoted by Br and Br*, respectively.

In the photolysis of NO_2 , it is to be expected that a non-monoenergetic distribution of O atom velocities will be obtained, corresponding to a distribution over the internal product states of $\text{NO}(X^2\Pi)$. Two related studies of NO_2 photodissociation,^{40,41} at wavelengths close to 355 nm, are apparently in contradiction over the details of the energy release,⁴¹ but both demonstrate a relatively broad distribution of O atom velocities, extending to the upper limit imposed by total energy conservation.

The energy available to be partitioned amongst the degrees of freedom of the products, $E_{O,NO}$, may be expressed as

$$E_{O,NO} = E(h\nu) - D_0^{\circ}(\text{NO}_2) + E_{\text{therm}}(\text{NO}_2) \quad (1)$$

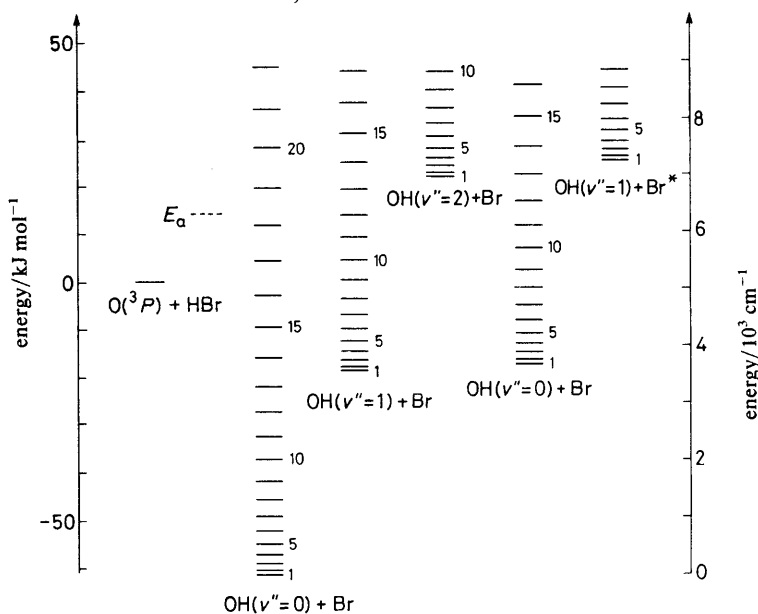


Fig. 6. Energetic diagram of reagent and product states in the $O(^3P) + HBr \rightarrow OH(X^2\Pi) + Br$ system. $^2P_{3/2}$ and $^2P_{1/2}$ bromine atom spin-orbit states are denoted by Br and Br*, respectively. E_a is the kinetically determined activation barrier.

where $E(h\nu) = 28\,190\text{ cm}^{-1}$ for third harmonic Nd:YAG radiation, $D_0^\circ(\text{NO}_2) = 25\,132\text{ cm}^{-1}$,⁴⁰ and $E_{\text{therm}}(\text{NO}_2)$ is the thermal translational and internal energy of NO_2 . Taking the limit where, in the photolysis, all the available energy appears as product translation, and assuming $E_{\text{therm}}(\text{NO}_2) = \frac{3}{2}kT$ (translation) + $\frac{3}{2}kT$ (rotation) = 620 cm^{-1} , conservation of linear momentum constrains the translational energy of the O atom, E_O , to be

$$E_O = \frac{1}{2} m_O v_O^2 = m_{\text{NO}} E_{O,\text{NO}} / (m_O + m_{\text{NO}}) = 2395\text{ cm}^{-1}, \quad (2)$$

where m_i and v_i are the mass and velocity, respectively, of species i .

Note that the production of electronically excited $O(^1D)$ is energetically impossible for single-photon dissociation of NO_2 at 355 nm. The absence of multiple-photon processes producing $O(^1D)$ under the present conditions was verified by a failure to observe any OH when photolysing NO_2 in the presence of H_2 ,⁴² or characteristically excited OH⁴³ in the presence of organic species [which produced only the rotationally 'cold' distributions previously reported¹³⁻¹⁹ for such systems in reactions with $O(^3P)$].

In the centre-of-mass frame of the $O + HBr$ collision, the collision energy, E_{coll} , may be approximated by

$$E_{\text{coll}} = \frac{1}{2} \mu (v_0^2 + 3kT/m_{\text{HBr}}) \quad (3)$$

where μ is the reduced mass of $O + HBr$ and the second term in parentheses represents the average contribution from thermal motion of HBr .⁴⁴ (In the present case, this term is almost negligible compared to v_0^2 .) Using the limiting value for v_0 derived above, a value of 2050 cm^{-1} is obtained for E_{coll} .

In addition to translational energy of the collision partners, the rotational energy of HBr is available to be partitioned between modes of the products. The QCT study of Persky and co-workers⁹ suggests that reactivity is substantially promoted by HBr rotation, and the average rotational energy of reactive HBr molecules is correspondingly significantly higher than that of the Boltzmann ensemble of reagents. Taking the value of

500 cm⁻¹ predicted by the QCT calculations for the average rotational energy of reactive HBr at 300 K, and a reaction exothermicity of 5150 cm⁻¹, an approximate limit to the total energy available to the products, relative to the lowest states of OH and Br, is deduced to be 7700 cm⁻¹.

Consideration of the measured OH product distributions in the light of fig. 6 and the discussion above clearly reveals that the majority of the energy available to the products appears as internal excitation of OH. The rotational distributions in $v'' = 1$ and 2 extend to $N'' = 16$ and 9, respectively, some 8300 and 8500 cm⁻¹ above the lowest level of $v'' = 0$. These energies exceed by several hundred cm⁻¹ the approximate energetic limit derived above, suggesting a significant contribution to reaction from states in the high-energy Boltzmann tail of the HBr rotational distribution. The peaks in the $v'' = 1$ and 2 distributions at $N'' \approx 12$ and $N'' \approx 5$, respectively, correspond to energies of 6300 and 7500 cm⁻¹.

The O(³P) + HBr reaction therefore exhibits dynamical behaviour quite distinct from that of the previously studied reactions of O(³P) with organic species, in which low levels of rotational excitation of the products were observed.¹³⁻¹⁹ In contrast, O + HBr displays properties characteristic of many H + LH' systems,¹⁻¹² in which the approximate propensity rule

$$E_{\text{trans}}(\text{reactants}) \approx E_{\text{trans}}(\text{products}) \quad (4)$$

(where E_{trans} is the kinetic energy), is obeyed in the selection of dominant product channels. This effect is essentially kinematic in origin. Relatedly, it has also been proposed⁴ that further propensity rules:

$$L(\text{reactants}) \approx L(\text{products}) \quad (5)$$

$$J(\text{reactant diatomic}) \approx J(\text{product diatomic}) \quad (6)$$

(where L and J refer to orbital and rotational angular momentum, respectively) would be obeyed if the reaction were uninfluenced by a controlling potential energy surface. Eqn (5) bears a close equivalence to eqn (4) in a direct H + LH' system. It has, however, been found^{1,12} that the conservation of rotational angular momentum expressed in eqn (6) is a relatively poor prediction, it being argued¹² that the product J is particularly sensitive to energy release controlled by the potential surface. The present experimental results do not allow a direct test of prediction (6), since the rotational distribution of reactive HBr molecules is unknown. However, only 0.2% of a 300 K sample of HBr occupies $J = 12$, the rotational angular momentum at the peak of the product OH($v'' = 1$) distribution, suggesting that a very dramatic increase in the reaction cross-section with HBr rotation would be required if propensity rule (6) were to be valid.

The above kinematic effects may alternatively be described using the vocabulary of potential-energy surfaces. In a mass-scaled coordinate system² the H + LH' mass combination exhibits a very narrow skewing angle between the entrance and exit valleys (this angle is 15.4° for O + HBr). The channelling of energy into the internal states of the products is then interpreted² as being the result of 'corner-cutting' trajectories, in which the much more rapid motion of the light compared to the heavy particles results in transfer of the light atom at relatively long range, before the equilibrium H---L internuclear separation is attained in the entrance channel.

As mentioned above, a quasiclassical trajectory study has recently been performed⁹ on a LEPS surface optimised to reproduce kinetic data for the O + HBr system. The surface derived has the barrier (of 13.2 kJ mol⁻¹) in the entrance channel, but is predominantly repulsive (the majority of the reaction exothermicity is released in the exit channel). The results of that study are not rigorously quantitatively comparable with those of the present experiments, since the calculations were performed for thermalised ensembles of reagents at various temperatures (200, 300 and 550 K). However, certain

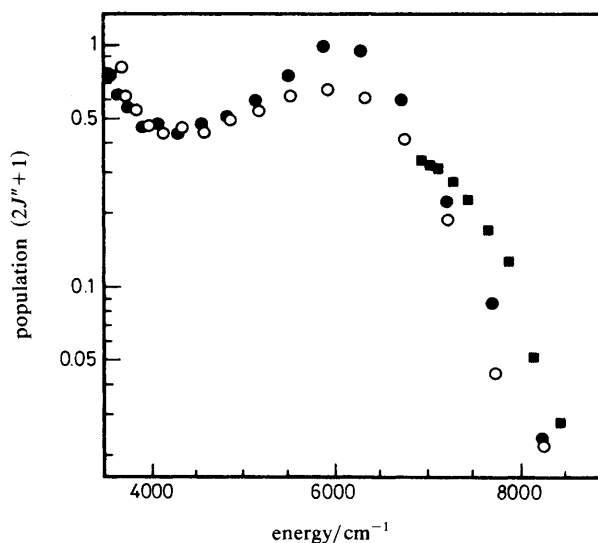


Fig. 7. Boltzmann plot of rotational state populations of OH($v'' = 1$ and 2) produced in the reaction O + HBr. ●, $v'' = 1$, $^2\Pi_{3/2}$ spin-orbit component; ○, $v'' = 1$, $^2\Pi_{1/2}$ spin-orbit component; ■, $v'' = 2$, $^2\Pi_{3/2}$ spin-orbit component.

enlightening comparisons are possible. The QCT studies correctly predict substantial vibrational and rotational excitation of OH. The predicted strong population inversion of $v'' = 1$ over $v'' = 0$, with 93% of OH in $v'' = 1$ for 300 K reagents, is highly consistent with the failure to observe nascent OH($v'' = 0$) in this study and in the previous e.s.r. experiments of Spencer and Glass.⁵ The average vibrational energy of the products (excluding zero-point energy) was *ca.* 40 kJ mol⁻¹ (almost independent of reagent temperature) in the QCT study, compared to 47 kJ mol⁻¹ in our experiments. Note, however, that no branching into $v'' = 2$ was predicted, in disagreement with the experimental observations. Experimentally, the average rotational energy (of $v'' = 1$ and 2) was 22 kJ mol⁻¹, falling between the predicted values of 18 and 23 kJ mol⁻¹ for reaction at temperatures of 300 and 550 K, respectively. It was also predicted that although the reaction cross-section does increase quite steeply with HBr rotation, the average rotational energy of the product OH is about three times greater than that of the reacting HBr molecules, consistent with the suggestion above that propensity rule (6) does not appear to be well obeyed in this system. No detailed product rotational state distributions were reported by Persky and coworkers.

An analysis of our experimental data was performed according to the 'surprisal' formalism,⁴⁵ in which measured distributions, $P_{\text{exptl}}(v'', N'')$, are compared with predicted prior distributions, $P_0(v'', N'')$, calculated solely on the basis of the density of available product states (neglecting angular momentum constraints). Plots of the surprisal function,

$$I(v'' = 1, N'') = -\ln [P_{\text{exptl}}(v'' = 1, N'') / P_0(v'' = 1, N'')] \quad (8)$$

were found to be highly non-linear. Such behaviour has been found elsewhere¹² in a computational study of a similar H + LH' system, Cl + HCl.

Interestingly, it was found that $I(v'' = 1, N'')$ for OH exhibited *two* extrema, in contrast to the single extremum of the Cl + HCl study.¹² This effect can also be discerned from fig. 7, where our experimental rotational distributions have been presented as a semilogarithmic plot of populations divided by the rotational degeneracy, $(2J'' + 1)$,

against the total internal energy. (This Boltzmann plot conveys information which is more limited but related to that of a surprisal plot, particularly at low internal energy where the density of available translational states is slowly varying, but has the advantage that the specification of an arbitrarily fixed total energy is avoided. The form of the surprisal of the more highly excited states is sensitive to this parameter, which is not well defined in our system.) The broad peak in fig. 7 at *ca.* 6000 cm^{-1} is characteristic of the type of behaviour also observed for $Cl + HCl$.¹² It is the subsidiary maximum at the lowest rotational state of $OH(v''=1)$ which we consider anomalous. [Note that this is *not* the result of partial relaxation of the measured distribution. Careful investigations at reduced values of $P\Delta t$ (see Experimental section, above) verified that the observed distribution was collisionally unmodified. Further strong support for this assertion is that the $OH(v''=2)$ data show no evidence for anomalous population of the lower rotational states.]

We suggest that this observation may be associated with the opening of an additional channel to form bromine atoms in the upper spin-orbit state, $^2P_{1/2}$. As fig. 6 shows, the $OH(v''=1) + Br^*$ channel lies slightly (some 280 cm^{-1}) above $OH(v''=2) + Br$, and hence is energetically accessible for $OH(v''=1, N'' \leq 7)$. This suggestion seems consistent with the character of the inflection in the $v''=1$ data of fig. 7. Although we have not attempted to obtain any direct experimental evidence for the occurrence of a minor channel producing Br^* , it is, in principle, an experimentally verifiable conjecture.

It can also be seen from fig. 7 that, in the vicinity of the higher N'' peak of the distribution, the $^2\Pi_{3/2}$ spin-orbit state of $OH(v''=1)$ is preferentially populated over $^2\Pi_{1/2}$, even when account is taken of the degeneracy differences (which are significant at low N'') and the data are plotted as a function of energy, rather than rotational quantum number. (No residual preference is apparent in the low N'' data.) A similar effect to that for the higher N'' levels was previously reported¹³ for the relatively unexcited distributions from reaction of $O(^3P)$ with organic systems. The argument presented by Andresen and Luntz¹³ to explain this observation was that the reaction was partially electronically adiabatic on surfaces correlating spin-orbit states of $O(^3P)$ with those of the $OH(X^2\Pi)$ product. The predominance of the lower, $^2\Pi_{3/2}$, state in OH was then essentially a consequence of the higher population of the lowest, 3P_2 , state of the reagent oxygen atoms, in thermal equilibrium from a microwave discharge source. Unfortunately, the distribution over the spin-orbit states of $O(^3P)$ produced by 355 nm photolysis of NO_2 is unknown, but it is rather intriguing, although possibly quite coincidental, that the OH spin-orbit ratio from the $O + HBr$ reaction under the present conditions is quite similar to that of the previous studies of organic systems.

The absence of any strong preference for either of the Λ -doublet substates is consistent with a direct, collinear mechanism of reaction. The possible slight discrepancy in favour of the $\pi(\perp J)$ state, near the peak of the $OH(v''=1)$ distribution, noted above, would be compatible with a tendency for these states to be produced *via* a bent reactive geometry, with an incipient bonding interaction between the O and Br atoms aligning the unpaired electron lobe on the O atom in the O—H—Br plane. Dynamical effects of this type, many of much greater magnitude, are well known in a number of other reactive systems.³⁹

In the discussion of the dynamics above, we have implicitly discounted the involvement of the deep potential well on the singlet surface which corresponds to the bound intermediate, $HOBr$. A spin-forbidden insertion mechanism, whereby an electronically non-adiabatic curve-crossing from the initial triplet surface would allow access to the singlet intermediate, seems a less satisfactory explanation for the observed results, given the very significant OH vibrational inversion and the highly non-linear rotational surprisals. These departures from statistical behaviour are more extreme than in previous systems where a short-lived intermediate complex is thought to be involved [e.g. $O(^1D) + HCl$ ⁴⁶ and $O(^1D) + H_2$ ⁴²].

Conclusion

The O + HBr reaction can be well understood in terms of a direct abstraction mechanism for a H + LH' system dominated by kinematic constraints. The highly inverted vibrational distribution results from an early barrier in the entrance channel, and 'corner-cutting' trajectories in which the H atom is transferred at relatively large internuclear distances. Substantial rotational excitation derives from repulsive interactions in the exit channel. Whilst the trajectory studies of Persky and co-workers⁹ are capable of at least good qualitative prediction of the observed product distributions using a LEPS surface with a collinear minimum-energy pathway, it seems clear that high rotational excitation of the products must result from repulsive Br...H interactions acting off the line of centres in a bent O—H—Br geometry. As has been discussed elsewhere,¹² the H + LH' mass combination channels this repulsive interaction very effectively into HL rotation, since the force acts on the L particle, with a long lever arm about the HL centre-of-mass. This suggests a possible explanation for the contrasting dynamics of O + organic systems compared to those of O + HBr, namely, that the O + organic systems may be subject to a stronger constraint towards collinearity, leading to much-reduced rotational excitation of the OH product.

We express our special thanks to two groups of workers; R. A. Copeland, J.B. Jeffries and D. R. Crosley, and M. Trolier and J. R. Wiesenfeld, for making available unpublished OH transition probabilities. (K.G.McK.) is grateful to the S.E.R.C. for the provision of a Postdoctoral Research Fellowship. This work was supported by the U.S. National Science Foundation under grant number NSF CHE 84-07270.

References

- 1 C. A. Parr, J. C. Polanyi and W. H. Wong, *J. Chem. Phys.*, 1973, **58**, 5.
- 2 J. C. Polanyi and J. L. Schreiber, in *Physical Chemistry, an Advanced Treatise*, ed. W. Jost (Academic Press, New York, 1974), vol. 6A, chap. 6, pp. 383-487.
- 3 M. Baer, *J. Chem. Phys.*, 1975, **62**, 305.
- 4 K. Schulten and R. G. Gordon, *J. Chem. Phys.*, 1976, **64**, 2918.
- 5 J. E. Spencer and G. P. Glass, *Int. J. Chem. Kinet.*, 1977, **11**, 97.
- 6 B. S. Agrawalla, A. S. Manocha and D. W. Setser, *J. Phys. Chem.*, 1981, **85**, 2873.
- 7 A. Persky and M. Broida, *J. Chem. Phys.*, 1984, **81**, 4352.
- 8 P. L. Gertitschke, J. Manz, J. Römel and H. H. R. Schorr, *J. Chem. Phys.*, 1985, **83**, 208.
- 9 M. Broida, M. Tamir and A. Persky, *Chem. Phys.*, 1986, **110**, 83.
- 10 A. Persky and H. Kornweitz, *Chem. Phys. Lett.*, 1986, **127**, 609.
- 11 P. M. Aker, D. J. Donaldson and J. J. Sloan, *J. Phys. Chem.*, 1986, **90**, 3110.
- 12 G. C. Schatz, B. Amaee and J. N. L. Connor, *Chem. Phys. Lett.*, 1986, **132**, 1.
- 13 P. Andresen and A. C. Luntz, *J. Chem. Phys.*, 1980, **72**, 5842.
- 14 K. Kleineremanns and A. C. Luntz, *J. Chem. Phys.*, 1982, **77**, 3533.
- 15 K. Kleineremanns and A. C. Luntz, *J. Chem. Phys.*, 1982, **77**, 3537.
- 16 K. Kleineremanns and A. C. Luntz, *J. Chem. Phys.*, 1982, **77**, 3774.
- 17 N. J. Dutton, I. W. Fletcher and J. C. Whitehead, *Mol. Phys.*, 1984, **52**, 475.
- 18 N. J. Dutton, I. W. Fletcher and J. C. Whitehead, *J. Phys. Chem.*, 1985, **89**, 569.
- 19 N. J. Barry, I. W. Fletcher and J. C. Whitehead, *J. Phys. Chem.*, 1986, **90**, 4911.
- 20 A. C. Luntz and P. Andresen, *J. Chem. Phys.*, 1980, **72**, 5851.
- 21 D. C. Clary, J. N. L. Connor and W. J. E. Southall, *J. Chem. Phys.*, 1986, **84**, 2620.
- 22 R. D. H. Brown and I. W. M. Smith, *Int. J. Chem. Kinet.*, 1975, **7**, 301.
- 23 D. J. Singleton and R. J. Cvetanovic, *Can. J. Chem.*, 1978, **56**, 2934.
- 24 D. F. Nava, S. R. Bosco and L. J. Stief, *J. Chem. Phys.*, 1983, **78**, 2443.
- 25 D. Arnoldi and J. Wolfrum, *Chem. Phys. Lett.*, 1974, **24**, 234.
- 26 R. D. H. Brown, G. P. Glass and I. W. M. Smith, *Chem. Phys. Lett.*, 1975, **32**, 517.
- 27 Z. Karny, B. Katz and A. Szöke, *Chem. Phys. Lett.*, 1975, **35**, 100.
- 28 R. G. Macdonald and C. B. Moore, *J. Chem. Phys.*, 1978, **68**, 513.
- 29 J. E. Butler, J. W. Hudgens, M. C. Lin and G. K. Smith, *Chem. Phys. Lett.*, 1978, **58**, 216.
- 30 G. H. Dieke and H. M. Crosswhite, *J. Quant. Spectrosc. Radiat. Transfer*, 1962, **2**, 97.
- 31 E. J. Shipsey, *J. Chem. Phys.*, 1973, **58**, 232.

- 32 R. Altkorn and R. N. Zare, *Annu. Rev. Phys. Chem.*, 1984, **35**, 265.
- 33 J. T. Yardley, in *Introduction to Molecular Energy Transfer* (Academic Press, New York, 1980), chap. 10.
- 34 R. A. Copeland, M. J. Dyer and D. R. Crosley, *J. Chem. Phys.*, 1985, **82**, 4022.
- 35 Rotational linestrengths were taken from: I. L. Chidsey and D. R. Crosley, *J. Quant. Spectrosc. Radiat. Transfer*, 1980, **23**, 187 and W. L. Dimpfl and J. L. Kinsey, *J. Quant. Spectrosc. Radiat. Transfer*, 1979, **21**, 233, except for off-diagonal bands for which values had not been reported, where the unpublished values of M. Trolier and J. R. Wiesenfeld were used.
- 36 C. H. Greene and R. N. Zare, *J. Chem. Phys.*, 1983, **78**, 6741.
- 37 R. Vasudev, R. N. Zare and R. N. Dixon, *J. Chem. Phys.*, 1984, **80**, 4863.
- 38 R. A. Copeland, J. B. Jeffries and D. R. Crosley, *Chem. Phys. Lett.*, in press.
- 39 P. Andresen and E. W. Rothe, *J. Chem. Phys.*, 1985, **82**, 3634.
- 40 G. E. Busch and K. R. Wilson, *J. Chem. Phys.*, 1972, **56**, 3626.
- 41 H. Zacharias, M. Geilhaupt, K. Meier and K. H. Welge, *J. Chem. Phys.*, 1981, **74**, 218.
- 42 C. B. Cleveland, G. M. Jursich, M. Trolier and J. R. Wiesenfeld, *J. Chem. Phys.*, 1987, **86**, 3253.
- 43 A. C. Luntz, *J. Chem. Phys.*, 1980, **73**, 1143.
- 44 E. E. Marinero, C. T. Rettner and R. N. Zare, *J. Chem. Phys.*, 1984, **80**, 4142.
- 45 R. D. Levine and R. B. Bernstein, *Acc. Chem. Res.*, 1974, **7**, 393.
- 46 A. C. Luntz, *J. Chem. Phys.*, 1980, **73**, 5393.

Received 7th May, 1987